

## Effects of Uniaxial Stress on the Absorption of the $F$ Center in KCl and the $U$ Center in $KBr^{\dagger*}$

ROBERT E. HETRICK<sup>†</sup>

*Department of Physics, University of Illinois, Urbana, Illinois 61801*

(Received 8 August 1969)

The stress-induced linear dichroism in the absorption of the  $F$  center in KCl and the  $U$  center in KBr has been measured in the range from 7 to 120°K. The moments analysis of Henry, Schnatterly, and Slichter has been used to interpret the results. For the  $F$  center, a measurement of the changes in the third moment of the  $F$  band allows the determination of the separate contributions to the second moment by lattice vibrations of  $\Gamma_1^+$ ,  $\Gamma_3^+$ , and  $\Gamma_5^+$  symmetry. Within the harmonic approximation, the temperature dependence of these separate contributions defines an average vibrational frequency for each symmetry mode broadening the band. The measured frequencies,  $\omega_1 = 2.3 \pm 0.1 \times 10^{13} \text{ sec}^{-1}$ ,  $\omega_3 = 1.95 \pm 0.1 \times 10^{13} \text{ sec}^{-1}$ , and  $\omega_5 = 1.4 \pm 0.1 \times 10^{13} \text{ sec}^{-1}$ , lie in the acoustic and low-frequency optical region of the host-lattice vibrational spectrum. The stress response for the  $U$  center was found to be qualitatively identical to that of the  $F$  center. The changes in the first moment of the  $U$  band determine the excited-state coupling to unit strains of  $\Gamma_3^+$  and  $\Gamma_5^+$  symmetry. From the changes in the third moment, it was found that cubic vibrations dominate the broadening of the  $U$  band. A broad peak in the dichroism pattern to the high-energy side of the  $U$  band is interpreted as evidence for transitions to higher excited states of the  $U$  center analogous to the  $K$ -band transitions associated with the  $F$  center.

### I. INTRODUCTION

IN 1965 both Schnatterly<sup>1</sup> and Gebhardt and Maier<sup>2</sup> reported on the response of the optical absorption of alkali-halide single crystals containing  $F$  centers to an applied uniaxial stress. Experimentally, they observed that the  $F$  and  $K$  bands (main absorption bands associated with the  $F$  center) exhibited a preferential absorption for light polarized parallel or perpendicular to the stress direction, depending on the excitation wavelength. The model for the  $F$  center is well established as that of an electron trapped at a negative ion vacancy. The site symmetry of the defect is cubic. Absorption arises due to excitation of the electron from its well-localized ground state of  $\Gamma_1^+$  symmetry to a series of excited states some of which lie near the conduction-band edge. The  $F$  band is associated with a dipole-allowed transition to a first excited state of  $\Gamma_4^-$  symmetry, while the  $K$  band is probably associated with a closely spaced set of higher excited states of  $\Gamma_4^-$  symmetry.<sup>3</sup> Within the framework of perturbation theory, the observed induced linear dichroism was analyzed in terms of either a stress splitting or mixing of these excited levels.

The work of Schnatterly followed directly from the development by Henry, Schnatterly, and Slichter<sup>4</sup> (hereafter denoted by HSS) of a method of analysis designed specifically to interpret the effects of small

perturbations on broad-band optical spectra. The  $F$  center is a representative if not a classic example of a center which exhibits this type of spectrum. Because of the strong interaction between the electronic states of the  $F$  center and the lattice, the  $F$ -absorption band is characterized by a near-Gaussian line shape, with a half-width at low temperature of approximately 0.2 eV.

Optical studies of such centers with applied fields must deal with both an experimental and theoretical problem arising from the broad-band property. From an experimental point of view, the magnitude of shifts or splitting of energy levels by an applied perturbation is usually small. For convenient magnitudes of stress, a good figure of merit is  $10^{-4}$  eV. Since such energy shifts are several orders of magnitude smaller than band half-widths, only small relative changes in line shapes occur. As a result, precise measurements of stress effects require the use of modulation techniques which can exploit the high gain of sensitive lock-in amplifiers. From a theoretical point of view, one would like to calculate the absorption line shape, include the effect on the perturbation, and calculate in detail any change in the line shape. This direct approach to analysis turns out to be quite difficult. As described by HSS, the main problem in the case of the  $F$  center lies in the degeneracy of the first excited state and the various perturbations which are present in the crystal. In addition to the electron-lattice interaction and the applied perturbation, the members of the excited multiplet are coupled by a significant spin-orbit interaction. Excluding the cesium halides, the spin-orbit splitting of the first excited state has been shown to be on the order of 0.01 eV.<sup>5</sup> HSS pointed out that the simultaneous coupling of the excited levels by noncubic lattice vibrations and the spin-orbit interaction can

<sup>†</sup> This work was supported in part by the National Science Foundation.

\* Based on a thesis submitted to the University of Illinois in partial fulfillment of the requirements for the degree of Doctor of Philosophy.

<sup>†</sup> Present address: Scientific Research Staff, Ford Motor Co., Dearborn, Mich.

<sup>1</sup> S. E. Schnatterly, Phys. Rev. **140**, A1364 (1965).

<sup>2</sup> W. Gebhardt and K. Maier, Phys. Status Solidi **8**, 303 (1965).

<sup>3</sup> D. Y. Smith and G. Spinolo, Phys. Rev. **140**, A2121 (1965).

<sup>4</sup> C. H. Henry, S. E. Schnatterly, and C. P. Slichter, Phys. Rev. **137**, A583 (1965).

<sup>5</sup> J. Mort, F. Luty, and F. C. Brown, Phys. Rev. **137**, A566 (1965).

lead to a breakdown in the Born-Oppenheimer or adiabatic approximation. As a consequence, there is ambiguity in calculating adiabatic potential curves for the excited state. Since this method for separating electron and lattice effects is usually crucial in making line-shape calculations, another technique not relying on this approximation is needed.

The method of HSS circumvents this difficulty by evaluating the first few moments of the absorption band, and the corresponding changes in these moments when the perturbation is applied. Paralleling somewhat the approach of Van Vleck in analyzing magnetic resonance line shapes,<sup>6</sup> the moments are expressed as diagonal sums over the excited-state wave functions. Such sums may be evaluated using any convenient bases for the excited state. Theoretically, the changes in the lower moments can be related to parameters of interest, while experimentally a numerical evaluation may be made from the dichroism data. Utilizing applied stresses, one can determine the first-excited-state coupling to static strains of various symmetries. In addition, one may determine the separate contributions to the broadening of the *F* band (as measured by the second moment) by three different symmetry lattice vibrations.

The present work extends that of Schnatterly in two ways. First, the stress response for the *F* band in KCl was measured as a function of temperature. Within the harmonic approximation, the temperature dependence of the separate contributions to the second moment defines an average vibrational frequency for the different symmetry modes which broaden the band. A comparison of these average frequencies with the phonon density of states of the host can then be made. Second, the stress measurements are extended to a new system, the *U* center in KBr. Consisting of a negative hydride ion at an anion site, the electronic structure and optical properties of the *U* center are quite similar to those of the *F* center. The present work allows a further comparison of these two systems on the basis of identical sets of stress parameters.

## II. GENERAL FEATURES OF *F* AND *U* CENTERS

### A. *F* Center

Figure 1(a) shows the *F*-center absorption spectrum in KCl at 7°K. Studied extensively in KCl, the *F*-band line shape can be empirically described as double Gaussian peaking in the green near 2.3 eV. The half-width of the band has a low-temperature value of  $H=0.169$  eV and is an increasing function of temperature. The simplest theory predicts a vibrationally broadened band whose half-width can be analytically described by

$$H^2(T) = H^2(0) \coth(\hbar\omega/2kT), \quad (1)$$

<sup>6</sup> J. H. Van Vleck, Phys. Rev. **74**, 1168 (1948).

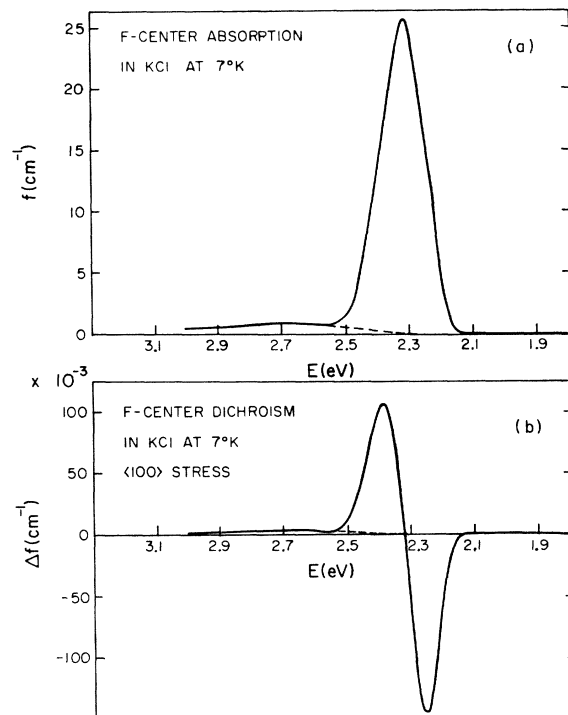


FIG. 1. (a) Optical absorption arising from *F* centers in KCl at 7°K. (b) *F*-center dichroism in KCl at 7°K for a  $\langle 100 \rangle$  stress.

where  $\omega$  represents an average vibrational frequency for all phonons broadening the band. This average frequency for the KCl *F* center ( $\omega=1.86 \times 10^{13}$  sec<sup>-1</sup>) as well as for several other host materials has been measured by Kuhnert and Gebhardt.<sup>7</sup> In most cases, the frequencies lie in the acoustic or low-frequency optical range of the host-material phonon density of states. The peak position of the band is also temperature-dependent, shifting to higher energy with decreasing temperature. Hydrostatic stress measurements suggest that most of this shift arises from thermal contraction.<sup>8</sup> Although the line shape has a marked temperature dependence, the area under the band has been found to remain constant with temperature, indicating that the oscillator strength is also a constant. Similar properties have been observed for the *F* band in other hosts. A recent and thorough review has been given by Markham.<sup>9</sup>

The *K* band appears as the absorption peak at the high-energy side of the *F* band. To even higher energy, and not shown in Fig. 1(a), are several weaker absorption bands, termed the *L* bands. The exact nature of the excited states associated with these transitions is not completely resolved.<sup>10</sup>

<sup>7</sup> H. Kuhnert and W. Gebhardt, Phys. Letters **11**, 15 (1954).

<sup>8</sup> I. S. Jacobs, Phys. Rev. **93**, 993 (1954).

<sup>9</sup> J. J. Markham, *F Centers in Alkali Halides* (Academic Press Inc., New York, 1966).

<sup>10</sup> F. Bassani and S. Guliano, in Proceedings of the International Symposium on Color Centers in Alkali Halides, Urbana, Ill., 1965 (unpublished).

### B. *U* Center

Figure 2(a) shows the absorption attributable to the *U* center in KBr at 78°K. Similar to the *F* center, the *U* center gives rise to a single prominent absorption band (*U* band) whose peak position has been shown to vary systematically with the lattice constant of the host (Ivey law). In KBr, the *U*-band peak absorption occurs near 5.5 eV. As for the *F* center, electronic levels of the *U* center are strongly coupled to the lattice, resulting in a broad absorption band with a near-Gaussian shape. The half-width of the KBr *U* band has a value of 0.25 eV at low temperature and increases with temperature in a manner similar to the *F*-band half-width. The high-energy tail of the *U* band overlaps appreciably with the exciton edge of the host, obscuring direct observation of absorption associated with higher excited states. Nevertheless, a careful subtraction of the optical densities measured in the *U*-band region, with and without the presence of the hydride ion, reveals the presence of a shoulder on the high-energy side of the *U* band. This shoulder may reasonably be attributed to a small absorption band peaking at 5.9 eV.<sup>11-13</sup> The appearance and position of the 5.9-eV band is strongly reminiscent of the *K*-band absorption associated with the *F* center. In their theoretical calculations, Wood and Opik<sup>14</sup> have observed

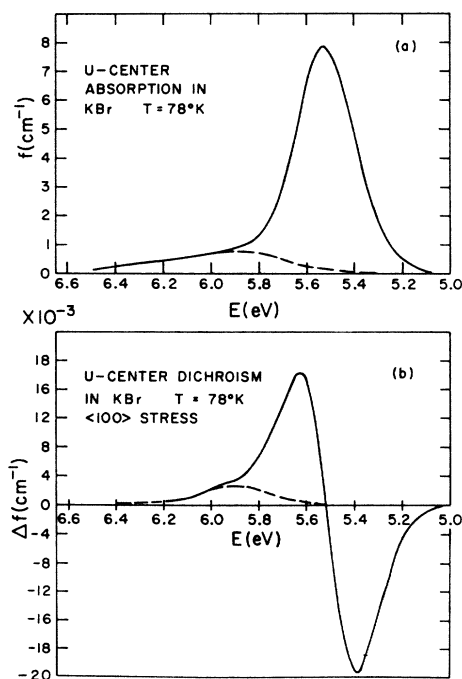


FIG. 2. (a) Optical absorption arising from *U* centers in KBr at 78°K. *U*-center dichroism in KBr at 78°K for a  $\langle 100 \rangle$  stress.

<sup>11</sup> H. Rockstad, Phys. Rev. **140**, A311 (1965).

<sup>12</sup> T. Goto, T. Ishii, and M. Ueta, J. Phys. Soc. Japan **17**, 1422 (1963).

<sup>13</sup> T. Timusk and W. Martienssen, Z. Physik **176**, 305 (1963).

<sup>14</sup> R. Wood and U. Opik, Phys. Rev. **162**, 736 (1967).

that the great similarity between the excited states of the *U* and *F* centers makes it likely that *K* and *L* bands are associated with both defects. The stress results to be presented later are consistent with and support this view.

There have been a number of theoretical studies of the *U*-center electronic structure beginning with the point-ion calculations of Gourary,<sup>15</sup> and, most recently, the extended-ion calculations of Wood and Opik<sup>14</sup> and Gilbert.<sup>16</sup> In each case, the *U*-band absorption is found to arise from a dipole-allowed transition between a ground state of  $\Gamma_1^+$  symmetry and a first excited state of  $\Gamma_4^-$  symmetry. Detailed calculations indicate a highly localized ground-state wave function and a first-excited-state wave function that overlaps appreciably with the second nearest neighbors of the hydride ion. Thus, in terms of symmetry and degree of localization, the electronic structure of the *U* center appears qualitatively identical to the *F* center. In this light, it is not surprising that the stress results for the two systems are similar. The moments analysis of HSS has been used in analysing the dichroism effects. As will be discussed later, however, the occurrence of isotope effects in the electronic absorption suggests that higher-order interactions associated with the *U*-center local vibrational mode, and not treated by HSS, are important and must be considered in making a detailed analysis of the stress results.

## III. STRESS EFFECTS ON *F* AND *U* CENTERS

### A. Qualitative Description

The *F* and *U* bands are broadened predominantly by lattice vibrations which can split or shift the first excited state. HSS have shown that only even-parity vibrations of  $\Gamma_1^+$  (cubic) and  $\Gamma_3^+$  and  $\Gamma_5^+$  (noncubic) symmetry participate in the broadening to first order. When a stress is applied, small static distortions occur which can be separated into these same symmetry types. For example, a  $\langle 100 \rangle$  stress produces strains of  $\Gamma_1^+$  and  $\Gamma_3^+$  symmetry. Using the  $(x,y,z)$  basis for the excited state, the  $\Gamma_3^+$  strain component (for stress along the *z* direction) produces a doublet (*x,y*), singlet (*z*) splitting of the excited state. Ignoring briefly certain complications due to the much larger dynamic distortions, one can view the absorption for transitions to such a split level as follows: For a beam incident along the *x* direction, the absorption band for *z*-polarized light will be shifted rigidly to higher energy, while that for *y*-polarization will shift to lower energy. A linear dichroism results, since *z*-polarized light is absorbed preferentially over the *y* polarization on the high-energy side of the band and vice-versa at lower energy. The dichroism experiment essentially measures the difference in absorption coefficient for these orthogonal polariza-

<sup>15</sup> B. S. Gourary, Phys. Rev. **112**, 337 (1958).

<sup>16</sup> R. F. Wood and R. Gilbert, Phys. Rev. **162**, 746 (1967).

tions of incident light. In the rigid-shift approximation, and for splittings small compared to the half-width, the dichroism pattern should have a shape identical to the derivative of the unstressed absorption line shape. Figures 1(b) and 2(b) illustrate the dichroism patterns for the  $F$  and  $U$  centers at 7 and 78°K, respectively, for a  $\langle 100 \rangle$  stress. The ordinate plots the difference in the line-shape function for light polarized parallel and perpendicular to the stress direction. It should be noted that the dichroism data are presented in terms of the line-shape function  $f(E)$ , which is defined as

$$\alpha(E) = CEf(E), \quad (2)$$

where  $\alpha(E)$  is the absorption constant.  $C$  is a proportionality constant whose form is discussed by HSS. Over the region of the  $F$ - and  $U$ -band absorption, both functions appear qualitatively identical.

The shape of the data in the  $F$ - and  $U$ -band regions closely resemble the derivative pattern suggesting the validity of the rigid-shift approximation. In addition, a weak broad peak occurs on the high-energy side of the main dichroism pattern for each center. For the  $F$  center, this peak corresponds to dichroism in the  $K$  band resulting from a stress mixing of the excited levels associated with the  $F$  and  $K$  bands. For the  $U$  center, a direct association of the high-energy peak with the 5.9-eV band observed in absorption seems unavoidable. The appearance of this peak and its similarity to the  $K$ -band dichroism is qualitative support for associating the 5.9-eV band with higher excited states of the  $U$  center. Quantitative support will be presented in Sec. V. For the principal bands, the magnitude of the dichroism in this case measures the excited-state coupling to a strain of  $\Gamma_3^+$  symmetry. By applying stress along a  $\langle 110 \rangle$  direction one can, in a similar manner, determine the coupling to strains of  $\Gamma_5^+$  symmetry. Strains of  $\Gamma_1^+$  symmetry do not produce dichroism; however, the coupling to this symmetry distortion can be obtained from hydrostatic stress measurements. Beyond these coupling coefficients, a careful analysis of the dichroism enables one to determine the separate contributions to the broadening of the  $F$  or  $U$  band by dynamic lattice modes of  $\Gamma_1^+$ ,  $\Gamma_3^+$ , and  $\Gamma_5^+$  symmetry. A detailed qualitative account of how this can be accomplished has been given by Schnatterly. Briefly, if the band is broadened only by lattice vibrations whose perturbation of the excited electronic level can be simultaneously diagonalized with the stress perturbation, then a uniform broadening results, and the rigid-shift approximation mentioned above holds. The derivative pattern is expected for the dichroism. For a  $\langle 100 \rangle$  stress, such a situation occurs if the band is broadened only by  $\Gamma_1^+$  and  $\Gamma_3^+$  lattice vibrations. If  $\Gamma_5^+$  dynamic distortions are present, however, the stress and lattice perturbations cannot be diagonalized simultaneously and wavefunction mixing occurs. This results in a skewing of the band and a deviation from the derivative pattern for

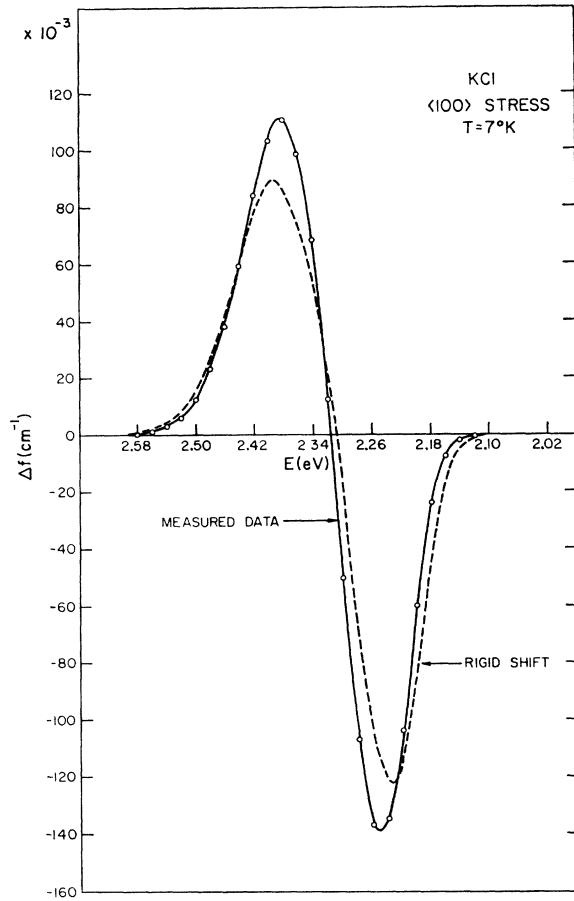


FIG. 3. Comparison of the measured dichroism pattern and the rigid-shift result for the  $F$  band in KCl at 7°K for a  $\langle 100 \rangle$  stress.

the dichroism. It is this deviation that is a measure of the extent to which  $\Gamma_5^+$  symmetry distortions broaden the band. Figure 3 illustrates this effect for the  $F$  band at 7°K. The plot is of the same form as Fig. 1(b), the solid curve indicating the measured data while the dashed curve is the rigid-shift result obtained directly from the derivative of the line shape. For these data, stress effects due to the  $K$  band have been subtracted from the total pattern so that the resulting dichroism is associated only with the  $F$  band. By analysing the differences between the rigid-shift and measured results for  $\langle 110 \rangle$  and  $\langle 100 \rangle$  stresses, the various symmetry contributions to the broadening may be determined.

## B. Moments Analysis

The above considerations are put on a quantitative basis through the moments analysis of HSS. The evaluation of the moments of the line shape in terms of parameters of interest is accomplished by adopting the following Hamiltonian for the system:

$$H = H_e(\mathbf{r}) + H_L(Q) + H'(\mathbf{r}, \mathbf{S}, Q), \quad (3)$$

where

$$H'(\mathbf{r}, \mathbf{S}, Q) = H_{eL}(\mathbf{r}, Q) + H_{SO}(\mathbf{r}, \mathbf{S}) + H_P(\mathbf{r}, Q). \quad (4)$$

For the  $F$  center,  $\mathbf{r}$  and  $\mathbf{S}$  represent the position and spin of the trapped electron, while  $Q$  is a generalized coordinate for the lattice.  $H_e(\mathbf{r})$  is the Hamiltonian for the trapped electron with the lattice at its equilibrium position.  $H_L(Q)$  represents the lattice in the harmonic approximation.  $H'(\mathbf{r}, \mathbf{S}, Q)$  consists of three terms which are treated as first-order perturbations on  $H_e(\mathbf{r}) + H_L(Q)$ .  $H_{eL}(\mathbf{r}, Q)$  is the linear electron-lattice interaction which couples defect electronic levels with the lattice motion.  $H_{SO}(\mathbf{r}, \mathbf{S})$  and  $H_P(\mathbf{r}, Q)$  represent the spin-orbit interaction and applied perturbation, respectively.

Direct calculation by HSS shows that the first moment can be written as

$$\bar{E} = E_\beta^0 - E_\alpha^0, \quad (5)$$

which is just the energy separation between the ground and first excited state in the unperturbed lattice. The usual parameter for measuring the broadening of a band is the half-width. In the moments analysis, the corresponding quantity is the second moment, which can be written as

$$\begin{aligned} \langle E^2 \rangle &= \langle E^2 \rangle_{eL} + \langle E^2 \rangle_{SO} \\ &= \langle E_1^2 \rangle + \langle E_3^2 \rangle + \langle E_5^2 \rangle + \langle E^2 \rangle_{SO}, \end{aligned} \quad (6)$$

where the separate contributions due to the different symmetry lattice modes are indicated. The spin-orbit contribution takes the form  $\langle E^2 \rangle_{SO} = \frac{1}{2}\lambda^2$ , where  $\lambda$  is the spin-orbit coupling constant. This quantity has been determined by circular dichroism measurements for KCl and is found to be  $\lambda = -6.7 \times 10^{-3}$  eV.<sup>5</sup>

In the same way for the third moment,

$$\langle E^3 \rangle = \langle E_1^3 \rangle + \langle E_3^3 \rangle + \langle E_5^3 \rangle + \langle E^3 \rangle_{SO}, \quad (7)$$

where  $\langle E^3 \rangle_{SO} = \frac{1}{4}\lambda^3$ .

The individual contributions to  $\langle E^2 \rangle_{eL}$  are proportional to the expectation value of the square of the appropriate lattice coordinate. In the harmonic approximation, this defines a characteristic temperature dependence given by

$$\begin{aligned} \langle E_\alpha^2(T) \rangle &= \langle E_\alpha^2(0) \rangle \coth(\hbar\omega_\alpha/2kT) \\ &\approx \langle E_\alpha^2(0) \rangle, \quad \text{for } kT \ll \hbar\omega_\alpha \\ &\approx \langle E_\alpha^2(0) \rangle 2kT/\hbar\omega_\alpha, \quad \text{for } kT \gg \hbar\omega_\alpha. \end{aligned} \quad (8)$$

In these expressions,  $\omega_\alpha$  represents an average vibrational frequency for each of the three types of vibrations. In a manner similar to that used in obtaining Eq. (1) for the half-width, one may also write a one-frequency formula as

$$\langle E^2(T) \rangle_{eL} = \langle E^2(0) \rangle_{eL} \coth(\hbar\omega_{av}/2kT), \quad (9)$$

where  $\omega_{av}$  represents a weighted average of the  $\omega_\alpha$ .

The third moment is found to be independent of

temperature and can be expressed in the one-frequency approximation by

$$\langle E^3 \rangle_{eL} = \langle E^2(0) \rangle_{eL} \hbar\omega_{av}. \quad (10)$$

This can be written in expanded form as

$$\langle E^3 \rangle_{eL} = \langle E_1^2(0) \rangle \hbar\omega_1 + \langle E_3^2(0) \rangle \hbar\omega_3 + \langle E_5^2(0) \rangle \hbar\omega_5. \quad (11)$$

When stress is applied, the expressions for the moments change with the inclusion of  $H_P(\mathbf{r}, Q)$  in the system Hamiltonian. In general, these changes are a function of the stress direction and the polarization of the incident light. For example, the differences between the first moment changes for parallel and perpendicular polarizations of the incident light for  $\langle 100 \rangle$  and  $\langle 110 \rangle$  stresses are

$$\langle \Delta E_{11} \rangle - \langle \Delta E_L \rangle = FA_3, \quad (12)$$

$$\langle \Delta E_{11} \rangle - \langle \Delta E_L \rangle = FA_5. \quad (13)$$

$F$  is the magnitude of the applied stress, and  $A_3$  and  $A_5$  are the excited-state coupling coefficients for unit strains of  $\Gamma_3^+$  and  $\Gamma_5^+$  symmetry (see Schnatterly for an exact definition of these quantities as matrix elements of  $H_P$  between excited-state wave functions).

The changes in the second moment of the band are proportional to the square of the appropriate coupling coefficients and are very small.

For a  $\langle 100 \rangle$  stress, the changes in the third moment are given by

$$\begin{aligned} \langle \Delta E_{11}^3 \rangle - \langle \Delta E_L^3 \rangle &= 3(\langle \Delta E_{11} \rangle - \langle \Delta E_L \rangle) \\ &\quad \times (\langle E_1^2 \rangle + \langle E_3^2 \rangle + \frac{1}{2}\langle E_5^2 \rangle + \frac{1}{4}\lambda^2), \end{aligned} \quad (14)$$

while for a  $\langle 110 \rangle$  stress

$$\begin{aligned} \langle \Delta E_{11}^3 \rangle - \langle \Delta E_L^3 \rangle &= 3(\langle \Delta E_{11} \rangle - \langle \Delta E_L \rangle) \\ &\quad \times (\langle E_1^2 \rangle + \frac{1}{2}\langle E_3^2 \rangle + \frac{5}{6}\langle E_5^2 \rangle + \frac{1}{4}\lambda^2). \end{aligned} \quad (15)$$

Provided the respective changes in the first moment are known, Eqs. (14), (15), and (6) for the second moment are sufficient to uniquely determine the separate contributions to the second moment. In this work, the temperature dependence of these different contributions has been measured and fit to the hyperbolic cotangent formula of Eq. (8), thus determining the average phonon frequencies  $\omega_1$ ,  $\omega_3$ , and  $\omega_5$ .

## IV. EXPERIMENTAL PROCEDURE

### A. Sample Preparation

#### 1. $F$ Center

$F$  centers were generated in Harshaw Chemical Co. KCl single crystals by x irradiation at 80°K. The x-ray tube utilized a tungsten target and was operated at 100 kV with a 25-mA filament current. Low-energy x rays were filtered from the beam with a copper plate, thereby insuring a uniform density of  $F$  centers across the width of the sample. Absorption measurements were made on a Cary 14R spectrophotometer. Neglig-

ible absorption was observed from *F*-aggregate centers. In most samples, the *F*-center concentration was on the order of  $10^{16} \text{ cm}^{-3}$ , as determined from Smakula's formula.

### 2. *U* Center

Alkali-halide crystals containing *U* centers were obtained by heating additively colored samples in a hydrogen atmosphere. Using an oscillator strength of unity, the *U*-center concentration was estimated to be on the order of  $10^{16} \text{ cm}^{-3}$ . Negligible optical bleaching of the *U* band occurred over the period of time required for the measurement of a complete dichroism pattern.

### B. Dichroism Apparatus

Dichroism measurements were made by passing monochromatic light through a rotating linear polarizer so that the sample repetitively saw equal intensities of light for all polarization directions. With the application of stress, the sample becomes dichroic, absorbing one of the incident polarizations preferentially over another. The intensity of the light leaving the sample and striking a photomultiplier tube was thus modulated at twice the frequency of the rotating polaroid. The magnitude of the intensity modulation was a direct measure of the induced dichroism. The corresponding modulation of the photomultiplier current was detected and amplified by a lock-in amplifier tuned to the proper frequency. Data were displayed on a strip-chart recorder.

In the visible region, pertinent optical components consisted of a quartz-iodine tungsten lamp as a light source, an RCA 7326 photomultiplier tube for light detection, and a Polaroid Corp. type H-32 linear polarizer. In the ultraviolet, a Kern-Springer 200-W hydrogen lamp was employed along with an EMI 9558Q photomultiplier tube. Wide-aperture ultraviolet polarizers utilizing organic films stretched on a quartz substrate were obtained from Polacoat Inc. These polarizers were found to be useful to  $0.2 \mu$ . At shorter wavelengths, the inherent absorption of the organic film limited their usefulness in the present application. Most measurements employed a Jarrell Ash 0.5-m monochrometer.

Measurements were made with crystals attached to a cold finger in an evacuated Sulfrin optical cryostat modified for stress measurements. Uniaxial stress was externally applied by means of a steel tube extending through the bottom of the cryostat. Internally, a series of three bellows was employed in transmitting the stress in order to preserve the vacuum and reduce the heat flux to the sample. When stress was applied, sample and cold finger came to thermal equilibrium near  $7^\circ\text{K}$  if liquid helium was the coolant. Higher temperatures could be obtained by means of a heater coil, an exchange gas column, and different coolants. Temperatures were monitored with a germanium resistance thermometer.

Quantitatively, the detection system is sensitive to the stress-induced change  $\Delta I$  in the intensity  $I$  of light

emerging from the sample. If  $\Delta I$  is small compared to the total intensity, this change can be linearly related to the difference  $\Delta\alpha$  between the defect's absorption coefficient  $\alpha$  for light polarized parallel and perpendicular to the direction of stress. At a given energy, let  $S(E)$  be the signal observed when a stress is applied to the crystal, while  $S_{\text{pol}}(E)$  is the signal obtained when a linear polarizer (with characteristics identical to those of the rotating polaroid) is inserted into the optical path. One can show in a straightforward manner that

$$l_1(\Delta\alpha_{\parallel} - \Delta\alpha_{\perp}) = \Delta I / I \sim S(E) / S_{\text{pol}}(E), \quad (16)$$

where  $l_1$  is the sample thickness, and the proportionality constant is determined by the relative adjustment of the photomultiplier anode current in the measurements of  $S(E)$  and  $S_{\text{pol}}(E)$ , and the efficiency of the polaroids. When the anode current is the same in both measurements, one has

$$l_1(\Delta\alpha_{\parallel} - \Delta\alpha_{\perp}) = \frac{2}{\coth\left[\frac{1}{2}(\alpha_2 - \alpha_1)l_2\right]} \frac{S(E)}{S_{\text{pol}}(E)}. \quad (17)$$

The hyperbolic cotangent accounts for deficiencies in the polaroids.  $\alpha_2$  represents the absorption coefficient of the polaroid for light polarized perpendicular to the pass axis, while  $\alpha_1$  is the corresponding quantity for light polarized along the pass axis. The width of the polarizer is denoted by  $l_2$ . Ideally  $\alpha_2 = \infty$  while  $\alpha_1 = 0$  and the value of the hyperbolic cotangent becomes unity. For real polarizers, the value of the hyperbolic cotangent is slightly greater than unity. The correction for this visible polarizer was negligible, but amounted to as much as 5% for the ultraviolet polarizer.

In a typical experiment,  $\Delta\alpha_{\parallel} - \Delta\alpha_{\perp}$  is measured at a series of wavelength intervals, and a dichroism pattern for a band is established. By means of Eq. (2), this quantity is related to  $\Delta f_{\parallel} - \Delta f_{\perp}$ , which is used in a numerical evaluation of the changes in the moments.

## V. EXPERIMENTAL RESULTS

### A. Data Treatment

For the *F* center, the primary data treatment involves eliminating the effects of the absorption and dichroism of the *K* band in order to obtain results representative of the *F* band only. Since the *K* band overlies the *F* band, the *K*-band absorption must be extrapolated into the *F*-band region and subtracted from the total absorption spectrum. This was done in a manner such that the slope of the resulting *F*-band line shape was a smooth function of energy. Schnatterly has studied the dichroism in the *K*-band region in detail and has shown that within certain reasonable approximations, it should have the same shape as the corresponding *K*-band absorption only shifted slightly to higher energy. Using this result, the *K*-band dichroism may also be subtracted from the total dichroism pattern.

The dichroism of interest arises solely from the

splitting of the first excited state. If the stress produces only a splitting, there should be no net change in the total transition probability for the transition that gives rise to the  $F$  band. As a consequence, the area under the dichroism pattern should be zero. After the  $K$ -band subtraction, however, the area under the dichroism pattern shows a small but nonzero value. This results primarily from a stress mixing of the  $F$ - and  $K$ -band excited levels. If mixing is assumed to occur uniformly at all energies, this effect can be eliminated by subtracting a curve from the pattern in the shape of the  $F$ -absorption band whose area equals the area change. The resulting pattern, which is used for numerical calculation, represents only the effects of the first-excited-state splitting. Figure 4 shows the corrected  $F$ -band dichroism for a  $\langle 100 \rangle$  stress at three different temperatures. The main feature is the increase in the magnitude of the peaks of the dichroism with decreasing temperature. This is consistent with the narrowing of the band on lowering the temperature. Another point is the shift of the zero of the pattern with decreasing temperature. This corresponds to the shifting of the peak of the band to higher energies as the temperature is lowered.

An exactly analogous situation requiring a similar treatment of the data occurs for the  $U$  center, if the absorption and dichroism of the 5.9-eV band are associated with higher excited states of the  $U$  center. Quantitative evidence that this is the case is obtained

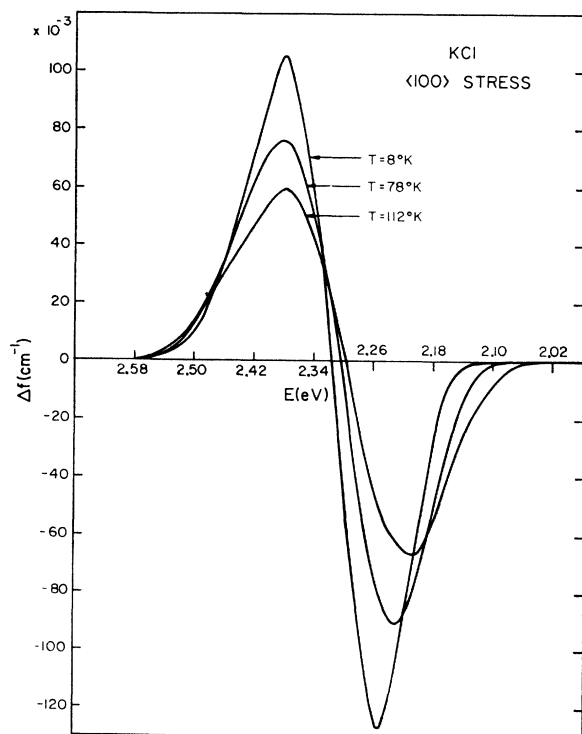


FIG. 4.  $F$ -band dichroism pattern in KCl at several different temperatures for a  $\langle 100 \rangle$  stress.

in the following way: In terms of the absorption coefficient  $\alpha(E)$  and the line-shape function  $f(E)$ , the statement of the oscillator strength sum rule<sup>17</sup> for transitions at a crystalline defect may be expressed as

$$\int_0^\infty \alpha(E) dE \sim \int_0^\infty E f(E) dE = \text{const.} \quad (18)$$

The second integral of Eq. (18) may be interpreted to read

$$A \bar{E} \simeq \text{const.} \quad (19)$$

Here,  $A$  is the area under the line-shape function for all dipole-allowed transitions from the ground state of the defect, while  $\bar{E}$  is the corresponding first moment of this extended absorption spectrum. To comply with the restrictions of Eq. (19), the observation of any small stress-induced change  $\Delta A$  in  $A$  implies a corresponding change  $\Delta E$  in  $\bar{E}$  in which these four quantities bear the relation

$$R = \frac{\Delta A}{A} / \frac{\Delta E}{E} \simeq -1. \quad (20)$$

Assuming that the 5.9-eV band is not associated with a transition from the  $U$ -center ground state, and subtracting the dichroism arising from this band from the measured pattern, the resulting values of  $\Delta A$  ( $\Delta A/A \simeq 7 \times 10^{-4}$  at 1 kg/mm<sup>2</sup>) and  $\Delta E$  produced by the stress combine to yield a value for the ratio  $R$  of  $R_U = -6.0 \pm 0.7$ . The subscript  $U$  in this case indicates that the result holds only for data taken in the  $U$ -band region. On the other hand, if one assumes that the 5.9-eV band arises from a transition to a higher excited state of the  $U$  center and correspondingly includes the dichroism in this region when evaluating  $R$ , then one finds values of  $\Delta A$  ( $\Delta A/A \simeq 10^{-4}$  at 1 kg/mm<sup>2</sup>) and  $\Delta E$  which produce a ratio  $R_{U,5.9} = -0.8 \pm 0.4$ . The subscript  $U,5.9$  indicates that the result holds for data taken in the composite  $U$ - and 5.9-eV band region. The improved agreement with the prediction of Eq. (20) on including the effects of the 5.9-eV band is additional support for the association of this band with the  $U$  center, and, in addition, argues that most of the oscillator strength for transitions from the  $U$ -center ground state is accounted for in the  $U$  and 5.9-eV bands. A completely analogous situation exists for the  $F$  and  $F$ - and  $K$ -composite bands.<sup>1</sup>

## B. Moments and Changes in Moments

### 1. $F$ Band

The first, second, and third moments of the  $F$  band were evaluated at a variety of temperatures over the range from 120 to 7°K. The area or zeroth moment was found to be independent of temperature within experimental error. The values of the first three moments at

<sup>17</sup> C. H. Henry and C. P. Slichter, in *Physics of Color Centers*, edited by W. B. Fowler (Academic Press Inc., New York, 1968), Chap. 6.

TABLE I. Values of the first, second and third moments of the *F* band in KCl and the *U* band in KBr.

<i>T</i> (°K)	$\langle E \rangle$ (eV)	$\langle E^2 \rangle_{eL}$ ( $10^{-3}$ eV <sup>2</sup> )	$\langle E^3 \rangle_{eL}$ ( $10^{-5}$ eV <sup>3</sup> )
78	2.308±0.001	5.74±0.20	8.1±0.4
7	2.320±0.001	4.33±0.20	7.5±0.4
78	5.518±0.002	17.2 ±0.9	11.3±2.1
7	5.521±0.002	12.5 ±0.8	10.9±2.1

78 and 7°K are listed in Table I. The first moment was found to increase monotonically with decreasing temperature in a manner similar to the shift in the peak of the band as measured by Konitzer and Markham.<sup>18</sup>

The various values of the second moment were fit to the single-mode formula of Eq. (9). The second moment at 7°K was chosen for the limiting value  $\langle E^2(0) \rangle_{eL}$ . The value of  $\omega_{av}$  was determined to be  $(2.05 \pm 0.1) \times 10^{13}$  sec<sup>-1</sup>.

The asymmetry of the *F* band is reflected in the size of the third moment. Although the moments analysis predicts no temperature dependence for this quantity, its value was found to decrease slightly with decreasing temperature. Part of this variation may be due to systematic errors in the *K*-band subtraction. Alternately, the moments analysis neglects such effects as nonlinear electron-lattice interactions, anharmonic lattice vibrations, and mixing of nondegenerate levels by the lattice. These effects have been discussed by Henry<sup>19</sup> and may lead to a temperature dependence of the third moment.

Stress-induced changes in the area of the *F* band have been discussed in Sec. V A. Values of  $A_3$  and  $A_5$  determined from changes in the first moment are listed in Table II at 78 and 7°K. These values agree well with

TABLE II. Values of the coupling coefficients  $A_1$ ,  $A_3$ , and  $A_5$  for the *F* band in KCl and KBr and the *U* band in KBr.

<i>T</i> (°K)	$A_1$ [ $10^{-4}$ eV/(kg/mm <sup>2</sup> )]	$A_3$ [ $10^{-4}$ eV/(kg/mm <sup>2</sup> )]	$A_5$ [ $10^{-4}$ eV/(kg/mm <sup>2</sup> )]
78	13.6±0.5 <sup>a</sup>	6.4±0.8	6.1±0.9 <sup>b</sup>
7		5.9±0.8	8.0±1.1
78	24.8 <sup>c</sup>	9.5±1.7	1.8±0.5
7		9.9±1.7	1.7±0.5
78	14.6±0.5 <sup>a</sup>	4.4±0.6 <sup>b</sup>	6.3±0.9 <sup>b</sup>

<sup>a</sup> Reference 8.

<sup>b</sup> Reference 1.

<sup>c</sup> Reference 20.

<sup>18</sup> J. D. Konitzer and J. J. Markham, J. Chem. Phys. 34, 1936 (1961).

<sup>19</sup> C. H. Henry, thesis, University of Illinois, 1965 (unpublished).

TABLE III. Separate symmetry contributions to the second moment of the *F* band in KCl.

<i>T</i> (°K)	$\langle E_1^2 \rangle$ ( $10^{-4}$ eV <sup>2</sup> )	$\langle E_3^2 \rangle$ ( $10^{-4}$ eV <sup>2</sup> )	$\langle E_5^2 \rangle$ ( $10^{-4}$ eV <sup>2</sup> )
78	31.1±3.5	10.2±1.2	16.2±1.9
7	25.2±2.3	6.1±0.8	12.0±1.1

those obtained by Schnatterly at 80°K. The magnitude of the coefficients was found to decrease slightly with temperature, but in each case the deviation was within the range of experimental error. This variation probably arises from an increase in the stiffness constants with decreasing temperature, although the temperature dependence of the local stiffness constants near the *F* center is unknown. As in the case of the third moment, the presence of the various interactions not included in the moments formulas can lead to a temperature dependence in  $\langle \Delta E \rangle$ . The magnitudes of these effects are also unknown.

The separate contributions to the second moment by the various symmetry lattice modes are listed in Table III at 78 and 7°K. At all temperatures, the  $\Gamma_1^+$  or breathing mode is dominant, constituting about 55% of the total second moment. Each set of values has been fit to Eq. (8) and the average frequencies  $\omega_\alpha$  obtained from an inverse hyperbolic cotangent versus  $1/T$  plot. The results are shown in Fig. 5. The frequency for the  $\Gamma_1^+$  mode is largest ( $\omega_1 = 2.3 \pm 0.1 \times 10^{13}$  sec<sup>-1</sup>) and

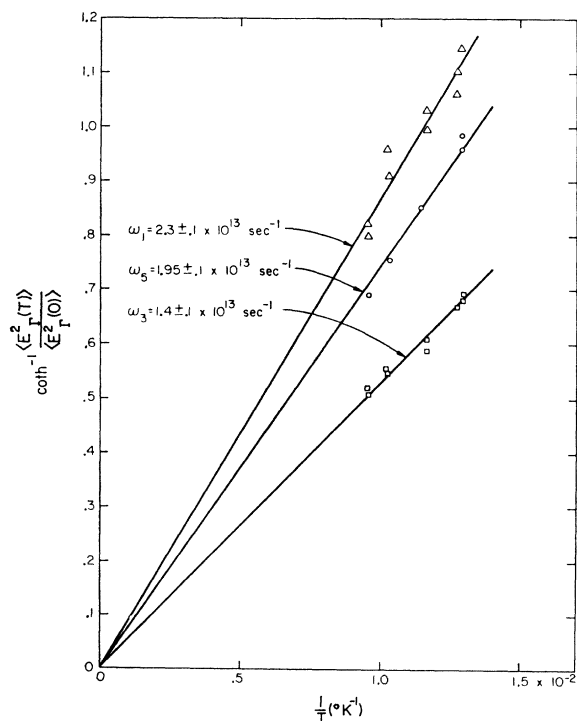


FIG. 5. Inverse hyperbolic cotangent versus  $1/T$  plot for obtaining the three values of  $\omega_\alpha$  from the temperature dependence of the separate contributions to the second moment of the *F* band.



decreases for the  $\Gamma_5^+$  ( $\omega_5 = 1.95 \pm 0.1 \times 10^{13} \text{ sec}^{-1}$ ) and  $\Gamma_3^+$  ( $\omega_3 = 1.4 \pm 0.1 \times 10^{13} \text{ sec}^{-1}$ ) modes, respectively.

## 2. *U* Band

The values of the first three moments of the *U* band are listed in Table I at 78 and 7°K. The area of the *U* band was found to be a constant function of temperature within an uncertainty of 2% of the measured value. The magnitude of the third moment was difficult to determine with good reliability, due to uncertainty in the exact shape of the high-energy tail of the *U* band resulting from the overlap with the exciton and 5.9-eV bands.

The first moment of the *U* band was found to increase monotonically with decreasing temperature in a manner similar to the first moment of the *F* band. Measurements of the pressure dependence of the *U*-band peak position at 78°K have been made by Lynch and Brothers.<sup>20</sup> They find  $(\partial E/\partial P)_T = 25.3 \times 10^{-6} \text{ eV/bar}$ , which in the context of the moments analysis corresponds to  $A_1 = 24.8 \times 10^{-4} \text{ eV/(kg/mm}^2\text{)}$ . The latter value is about twice that observed for the *F* band in KBr. Baldini, Mulazzi, and Terzi<sup>21</sup> have studied the temperature dependence of the *U*-band peak position in three alkali halides. In the range from 4 to 300°K in KBr they fit

their results by the relation  $\bar{E} = E_0 - B \coth(\hbar\omega/2kT) + C$ , where  $B = 0.04 \text{ eV}$  and  $\omega_1 = 2.36 \times 10^{13} \text{ sec}^{-1}$ . Lynch and Brothers<sup>22</sup> have shown that the measurements of both the temperature  $(\partial E/\partial T)_P$  and pressure  $(\partial E/\partial P)_T$  coefficients of an impurity absorption peak enables one to determine the separate contributions of the electron-lattice interaction and thermal contraction to the observed temperature variation of the peak position. Using the experimental results given above and the bulk values for the thermal-expansion coefficient and isothermal compressibility, one finds that thermal contraction contributes approximately 80% to the observed temperature dependence of the peak position in KBr.<sup>20</sup>

From the temperature dependence of the total second moment, an average vibrational frequency [ $\omega_{av} = (1.9 \pm 0.15) \times 10^{13} \text{ sec}^{-1}$ ] was found for all phonons broadening the *U* band. This agrees within experimental error with the average frequency obtained from the temperature variation of the half-width.

The changes in the *U*-band moments were obtained as for the *F* band. Figure 6 illustrates the stress results (uncorrected for the 5.9-eV band) at several different temperatures. The main features of the temperature dependence are identical for the *F* and *U* bands. Values of  $A_3$  and  $A_5$  at 78 and 7°K as determined from changes in the first moment are listed in Table II along with those determined by Schnatterly for the KBr *F* band. For each system, the order of magnitude of the coefficients is the same, although  $A_3$  is substantially larger than  $A_5$  for the *U* band. A discussion of the changes in the third moment is deferred until Sec. VI.

## VI. DISCUSSION

### A. *F* Center

The main result for the *F* center is the determination of the average vibrational frequencies  $\omega_\alpha$ . A comparison of these frequencies with the phonon density of states bears on the difficult problem of how lattice defects or impurities perturb the vibrational spectrum of the host lattice. Unfortunately, the phonon density of states in KCl has not yet been experimentally determined; however, as for most alkali halides, Karo and Hardy<sup>23</sup> have performed extensive calculations of this quantity based on the deformation dipole model for the lattice. Their phonon distribution for KCl at 0°K shows a continuous spectrum beginning with a Debye region at lowest frequencies and continuing through two peaks in the range of acoustic frequencies and a large peak corresponding to the main TO frequency ( $2.9 \times 10^{13} \text{ sec}^{-1}$ ). A comparison of the  $\omega_\alpha$  with these results indicates that the average frequencies for phonons broadening the *F* band do not correspond to particular peaks in the host density of states, but that they do

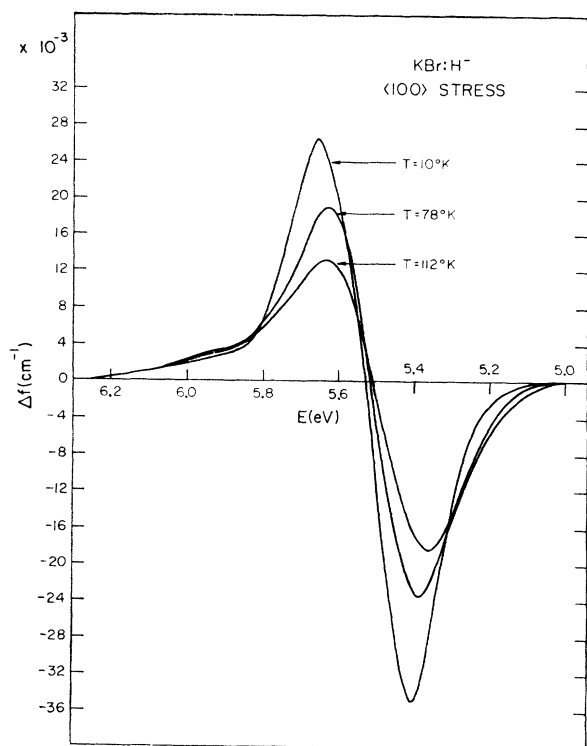


FIG. 6. *U*-center dichroism pattern in KBr at several different temperatures for a (100) stress.

<sup>20</sup> A. Brothers and D. Lynch (private communication).

<sup>21</sup> G. Baldini, E. Mulazzi, and N. Terzi, Phys. Rev. **140**, A2094 (1965).

<sup>22</sup> A. Brothers and D. Lynch, Phys. Rev. **164**, 1124 (1967).

<sup>23</sup> A. M. Karo and J. R. Hardy, Phys. Rev. **129**, 2024 (1963).

ie in the lower-frequency acoustic region of the spectrum.

Calculations of the effect of  $F$  centers in NaCl on the vibrational spectrum near the defect have been made by Matthew, McCombie, and Murray.<sup>24</sup> Reducing the problem to a normal mode calculation, they consider the  $\Gamma_1^+$  symmetry vibrations of the ions in the first 11 shells surrounding the  $F$  center with all other ions being fixed. They then calculate the frequency distribution of these normal modes with and without the repulsive potential of one of the negative ions. The two situations correspond to a lattice with and without an  $F$  center. It was found that the presence of the  $F$  center greatly increased the amplitude of the low-frequency vibrations while reducing the amplitudes of the higher-frequency vibrations. At the same time the frequencies of the perturbed modes were not shifted greatly from those obtained for the perfect lattice. The three frequencies obtained from the stress results offer a similar but more restricted comparison of the two situations in KCl. In this case also, it appears that the effect of the higher-frequency optical vibrations has been reduced. The dynamic distortions broadening the  $F$  band seem to be either perturbed phonons or resonance modes lying in the acoustic-phonon frequency region.

Several additional techniques may be used to determine the frequencies of the phonons perturbing the  $F$  band. Most recently, Henry<sup>25</sup> has shown that by measuring the polarized Raman scattering from  $F$  centers one may determine, within certain approximations, the entire frequency spectrum for each of the three types of symmetry vibrations. Measurements of the Raman spectrum for  $F$  centers in KCl and NaCl have been made by Worlock and Porto<sup>26</sup> at liquid-nitrogen temperature. Their data show that the  $F$  center in KCl couples with a wide spectrum of frequencies ranging from  $7.5 \times 10^{12}$  to  $3.7 \times 10^{13}$  sec<sup>-1</sup>. Peaks in the Raman spectrum are very broad, but the one occurring near  $1.5 \times 10^{13}$  sec<sup>-1</sup> may correspond to the frequency  $\omega_3$  of the  $\Gamma_3^+$  symmetry vibrations determined by the dichroism results. High-resolution low-temperature Raman spectra have recently been reported by Buchenauer *et al.*<sup>27</sup> for the  $F$  center in NaBr. Measurements of similar accuracy would be useful in KCl.

Very recently, Benedek and Mulazzi<sup>28</sup> have made a detailed calculation of the Raman scattering spectra from the  $F$  center in KCl and other materials at 78°K. They use the deformation dipole model for the lattice and take into account local force-constant changes due to the defect. Their results indicate that  $\Gamma_3^+$  symmetry

vibrations contribute strongly to the scattering at a frequency very near that assigned to  $\omega_3$  in this work. The influence of  $\Gamma_1^+$  and  $\Gamma_5^+$  modes were found to cover a wider range of frequencies. Without a detailed comparison, the weighted average for these frequencies would appear to be in reasonable agreement with the values of  $\omega_1$  and  $\omega_3$  determined from the stress data.

In conclusion, it should be noted that the one- and three-frequency formulas for the third moment [Eqs. (10) and (11)] enable one to perform a rough check on the consistency of the analysis. Using the measured values of the separate contributions to second moment along with the corresponding average frequencies, one may calculate the third moment of the band  $\langle E^3 \rangle_{eL}^{calc}$ . This in turn can be compared with the measured value. Using the one-frequency formula, Schnatterly found a deviation of 34.3% between the calculated and measured values for KCl. Using the three-frequency formula and the low-temperature value for the measured third moment, this deviation is reduced to 19.0%, with  $\langle E^3 \rangle_{eL}^{calc} = 5.91 \times 10^{-5}$  eV<sup>3</sup>. The deviation remains substantial and probably reflects the influence of the previously mentioned approximations used in the analysis.

#### B. $U$ Center

The interpretation of the changes in the higher moments of the  $U$  band is complicated due to isotope effects studied by Baldini *et al.*<sup>21</sup> In the three alkali halides studied, they find that the substitution of  $D^-$  for  $H^-$  ions results in both a shift of the peak position of the  $U$  band to higher energy and a decrease in the half-width of the band. Since lattice modes involving the impurity ion are of odd parity, they do not participate to first order in band broadening via energy-level splittings. Hence, isotope effects suggest that higher-order processes contribute substantially to the  $U$ -band broadening. This is the interpretation of Baldini *et al.*,<sup>21</sup> who analyse the isotope effects in terms of the change in the frequency of the  $U$  center's local vibrational mode (frequency effect<sup>29</sup>) during the electronic transition. Qualitatively, the redistribution of electronic charge in the excited state weakens local force constants, thus reducing vibrational frequencies. For example, they find that in order to fit their data, the local mode frequency of the  $H^-$  ion in KBr must be reduced by a factor near 2 on going from the ground to first excited state. A similar reduction is required for the  $D^-$  ion local mode. Assuming a Gaussian band shape and using the Condon approximation, these changes enter into expressions for the peak position and half-width in such a manner as to account for both the magnitude and temperature dependence of the isotope effects. Using their formalism and values for the frequency changes, one finds that the frequency effect for the  $H^-$  ion local mode contributions approximately 6% to the total

<sup>24</sup> C. W. McCombie, J. A. D. Matthew, and A. M. Murray, *J. Appl. Phys.* **33**, 359 (1962).

<sup>25</sup> C. H. Henry, *Phys. Rev.* **152**, 669 (1966).

<sup>26</sup> J. M. Worlock and S. P. S. Porto, *Phys. Rev. Letters* **15**, 697 (1965).

<sup>27</sup> C. J. Buchenauer, D. B. Fitchen, and J. B. Page, Jr., *Abstract No. 31*, International Symposium on Color Centers in Alkali Halides, Rome, Italy, 1968 (unpublished).

<sup>28</sup> G. Benedek and E. Mulazzi (private communication).

<sup>29</sup> Y. E. Perlin, *Usp. Fiz. Nauk* **80**, 553 (1963) [English transl.: *Soviet Phys.—Usp.* **6**, 542 (1964)].

half-width of the  $U$  band in KBr. Unfortunately, no direct experimental evidence exists that such large changes occur in the local mode frequency when the  $U$  center is in its excited state.

Theoretical interest leading to alternative explanations of the isotope effect persists. For example, Matthew and Hart-Davis<sup>30</sup> have examined the relative importance of band and localized modes in quadratic terms of the electron-lattice interaction. Interactions involving localized modes are found to dominate, allowing for the possibility of strong isotope effects. Alternately they note that the mean-square displacements of the  $H^-$  and  $D^-$  ions acting as Einstein oscillators are widely different due to the large relative mass difference. This could have a significant effect on the frequency of vibrational modes of neighboring ions if the anharmonic coupling between the impurity and host lattice is strong. Such frequency changes could account for the isotope effect in the half-width of the  $U$  band. More recently, Mitra *et al.*,<sup>31</sup> utilizing a configuration coordinate model, find that band mode optical phonons are dominant in the  $U$ -band broadening. As a consequence, they indicate that the isotope effects can be explained without involving the participation of localized modes. The results of the stress experiments alone are insufficient to discriminate among these various possibilities, since a generalization of the moments analysis to include higher-order electron-lattice interactions or anharmonic effects leads to a large number of parameters which cannot be separately determined.

Although the interactions leading to the isotope effects are significant, they do not dominate the absorption spectrum of the  $U$  center. In analysing the stress results, one expects that those parameters defined by expressions in the moments analysis which do not depend on the linear electron-lattice interaction (such as  $A_3$  and  $A_5$ ) will be largely unaffected by higher-order interactions. On the other hand, the changes in the third moment as given by Eqs. (14) and (15) depend strongly on the electron-lattice interaction, and parameters derived from these expressions cannot be unambiguously interpreted with the same certainty as for the  $F$  center. Nevertheless, it was thought worthwhile to perform the third moment analysis to determine whether the noncubic lattice vibrations make a large or small contribution to the  $U$ -band broadening. It was found, in contrast to the  $F$ -center results, that for temperatures up to 120°K  $\langle E_1^2 \rangle / \langle E^2 \rangle_{eL} \approx 1.0 \pm 0.15$ . The indicated error is experimental. For a  $\langle 100 \rangle$  stress, a large portion of the error results from ambiguity in subtracting the 5.9-eV band dichroism. For a  $\langle 110 \rangle$  stress, statistical error becomes important because of

the small magnitude of the stress response. This is reflected in the fact that  $A_5$  is nearly five times smaller than  $A_3$ .

Justification for the relative magnitudes of the cubic and noncubic contributions to the second moment requires a detailed knowledge of the coupling of the energy levels to each of the relevant vibrational modes, and the corresponding frequency distribution of these modes. The nonzero values of  $A_3$  and  $A_5$  measure the extent and relative magnitude of the coupling of the  $U$ -band excited state to long-wavelength acoustic phonons of noncubic symmetry. To the extent that this type of phonon contributes to the broadening, one would expect to detect the noncubic contributions to the second moment unless the coupling to cubic distortions (measured by  $A_1$ ) is substantially larger.

The correlation between second moment contribution and coupling coefficient is illustrated on a qualitative scale by the  $F$ -center results. It is felt that the longer-wavelength acoustic phonons contribute strongly to the  $F$ -band broadening. Further, the cubic vibrations invariably contribute more than 50% of this broadening. Correspondingly, the coupling coefficient  $A_1$  for static cubic distortions is always larger (by a factor of 2 to 4) than those for the noncubic static distortions. The correspondence between the long-wavelength coupling coefficient and second moment contribution should, of course, break down as higher-frequency optical phonons take on increased importance in the broadening.

A comparison of the frequency  $\omega_{av}$  with the phonon density of states in KBr indicates that acoustic phonons probably contribute substantially to the broadening of the  $U$  band. In addition, the density of states of perturbed lattice phonons which may couple anharmonically with the hydride ion ionic motion has been calculated<sup>32</sup> in order to predict the sideband structure of the infrared absorption produced by the  $U$  center. These calculations indicate an increased density of states in the low-frequency range of the phonon spectrum when  $U$  centers are present. In view of these remarks, the dominance of cubic vibrations in the broadening of the  $U$  band and the fact that  $A_1$  is larger than either  $A_3$  or  $A_5$  are at least consistent experimental observations.

Additional confirmation that the contribution of  $\Gamma_5^+$  symmetry vibrations is small is given in Fig. 7. In this plot, the measured and rigid-shift results are shown for a  $\langle 100 \rangle$  stress at 78°K. As expected from the discussion of Sec. III A, the shape of the measured data is virtually identical with that of the derivative of the unstressed absorption band. This is consistent with a large cubic contribution to the broadening. This plot should be compared with that in Fig. 3 for the  $F$  center, where the

<sup>30</sup> J. A. D. Matthew and A. Hart-Davis, Phys. Rev. **168**, 936 (1968).

<sup>31</sup> S. S. Mitra, R. S. Singh, and Y. Brada, Bull. Am. Phys. Soc. **14**, 131 (1969).

<sup>32</sup> T. Timusk and M. V. Klein, Phys. Rev. **141**, 664 (1966).

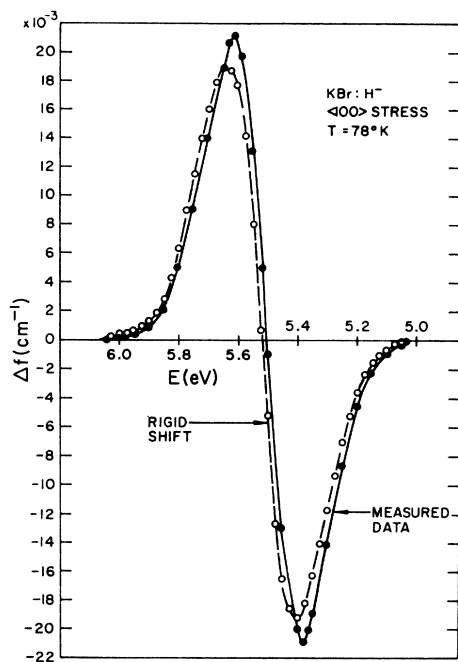


FIG. 7. Comparison of the measured dichroism pattern and the rigid-shift result for the  $U$  band in KBr at  $78^\circ\text{K}$  for a  $\langle 100 \rangle$  stress.

large contribution of the  $\Gamma_5^+$  modes leads to a marked deviation between the measured and rigid-shift patterns.

In Fig. 7, the rigid-shift result appears displaced slightly to higher energy rather than coincident with the measured data. If only cubic vibrations (and in this case tetragonal vibrations also) contribute to the broadening, one would expect that the results of the expansion leading to the rigid-shift curve (derivative pattern), if carried to sufficiently high order, should duplicate exactly the measured result. The first higher-order correction to the rigid-shift result takes on the form  $\langle \Delta E_1 \rangle \langle \Delta E_3 \rangle (\partial^2 f(E) / \partial E^2)$ , where  $\langle \Delta E_1 \rangle$  and  $\langle \Delta E_3 \rangle$  refer to the change in the first moment due to  $\Gamma_1^+$  and  $\Gamma_3^+$  symmetry distortions, respectively. Using the known values for these quantities, such a correction term does in fact improve the agreement between the measured and "calculated" patterns, although it is not of sufficient magnitude to bring about coincidence within experimental error. The remaining disagreement between the curves presumably results from a small but nonzero contribution to the broadening by  $\Gamma_5^+$  symmetry vibrations, or systematic errors in the subtraction of the 5.9-eV band absorption and dichroism patterns. A similar comparison between the rigid-shift result and the measured data holds for the case of  $\langle 110 \rangle$  stresses, indicating that the contribution of  $\Gamma_3^+$  symmetry vibrations to the broadening of the  $U$  band is not large.

## VII. SUMMARY

The  $F$  center in KCl and the  $U$  center in KBr have been studied by observing the response of their absorption spectra to an applied uniaxial stress. In particular, the stress-induced linear dichroism in the absorption has been measured. Utilizing the moments analysis of HSS, the stress results have been analyzed in the framework of perturbation theory yielding parameters which characterize the center and its interaction with the host lattice. Both centers possess broad absorption bands arising from electronic levels that are interacting strongly with local lattice vibrations. As a result, the lattice must be treated in detail in analysing the results of perturbation experiments. Consequently, for applied stresses, in addition to parameters which measure the coupling of electronic levels to static distortions of the lattice, one may also obtain information on the dynamic distortions and how they are perturbed by the defect.

For the  $F$  center, the original measurements of Schnatterly have been extended to include the temperature dependence of the stress effects in KCl. By measuring the changes in the third moment of the band, the separate contributions to the broadening of the band (as measured by the second moment) by  $\Gamma_1^+$ ,  $\Gamma_3^+$ , and  $\Gamma_5^+$  symmetry vibrations can be determined. The temperature dependence of these parameters defines an average vibrational frequency for each symmetry mode. A comparison of the measured frequencies with the calculated phonon density of states for KCl indicates that the lattice distortions which couple to the  $F$ -center electronic levels may be either perturbed or resonance phonons lying primarily in the acoustic range of the host vibrational spectrum.

The stress results and their temperature dependence for the  $U$  band are qualitatively identical to those for the  $F$  band. The first excited state coupling to static distortions of  $\Gamma_3^+$  and  $\Gamma_5^+$  symmetry was determined to be of the same order as that for the  $F$  band. It was found that the contribution to the broadening of  $U$  band by lattice vibrations of cubic symmetry was much larger than for noncubic vibrations. A weak broad peak in the dichroism pattern on the high-energy side of the  $U$ -band peak position was interpreted as evidence for transitions to higher-excited states of the  $U$  center, in analogy to the  $K$ -band transitions associated with the  $F$  center.

## ACKNOWLEDGMENTS

It is the author's pleasure to acknowledge the guidance and assistance of his thesis advisor, Professor W. Dale Compton, throughout the course of this work. The author is also grateful to Dr. W. J. Burke, Dr. J. A. Borders, and D. Y. LeCorgne for their generous assistance and helpful discussions on various aspects of this investigation.